Analytical Functions Used for Description of the Plastic Deformation Process in Zirconium Alloys WWER Type Fuel Rod Cladding under Designed Accident Conditions

P. Fedotov

A. A. Bochvar All Russian Research Institute of Inorganic Materials, Moscow, Russian Federation

1. Introduction

Substantiation of nuclear fuel safety is important for it's licensing. For calculation substantiation of the WWER type fuel rod under designed accident conditions the RAPTA-5 code is used [1].

The aim of this work was to improve the RAPTA-5 code as applied to the analysis of the thermomechanical behavior of the fuel rod cladding under designed accident conditions. The irreversible process thermodynamics methods were proposed to use for the description of the plastic deformation process in zirconium alloys under accident conditions. Functions, which describe yielding stress dependence on plastic strain, strain rate and temperature may be successfully used in calculations.

2. Analytical Function

In [2] it was suggested to use the irreversible process thermodynamics methods for the description of the plastic deformation process under different conditions (temperature, strain rate).

The yielding stress dependence on plastic strain, strain rate and temperature is as follows (1):

$$\sigma = \sigma_0 \cdot Z_T \cdot Z_{\dot{\varepsilon}} \cdot Z_\varepsilon \quad (1)$$

where:

σ_0 – yield stress under temperature equal 0 K and strain rate is $\dot{\varepsilon}_0$,

Z_T – temperature factor,

$Z_{\dot{\varepsilon}}$ – strain rate factor,

Z_ε – deformation strengthening factor.

$$\sigma_T = \sigma_0 \cdot Z_T \cdot Z_{\dot{\varepsilon}} \quad (2)$$

where σ_T is yield stress.

Temperature factor depends on the temperature like exponential curve (3):

$$Z_T = e^{-bT} \quad (3)$$

where *b* is constant.

Strain rate factor depends on strain rate like power dependence (4):

$$Z_{\dot{\varepsilon}} = \left(\frac{\dot{\varepsilon}}{\dot{\varepsilon}_0}\right)^a \quad (4)$$

where *a* is exponent of power (5):

$$a = C_{1a} + C_{2a} \cdot T \quad (5)$$

where $C_{1\alpha}$, $C_{2\alpha}$ is constants.

Deformation strengthening factor is as follow function (6):

$$Z_\varepsilon = e^{m\cdot(1-\eta^\nu)} \quad (6)$$

where *m* – coefficient of strengthening,

$$\eta = 1 + \varepsilon,\ \varepsilon = \ln\frac{L}{L_0},$$

ν is index of strengthening (7,8):

$$m = (C_{1m} + C_{2m} \cdot T)\left(1 + C_{3m} \cdot \lg\left(\frac{\dot{\varepsilon}}{\dot{\varepsilon}_0}\right)\right) \quad (7)$$

$$\nu = C_{1\nu} \cdot \left(\frac{\dot{\varepsilon}}{\dot{\varepsilon}_0}\right)^{C_{2\nu}} \quad (8)$$

where C_{1m}, C_{2m}, C_{3m}, $C_{1\nu}$, $C_{2\nu}$ are constants.

Ta date there is an experience of use of function (1) for the description of the plastic deforming of E110 and E635 alloys in the low temperatures area [3-5].

3. Yield Stress Temperature Dependence

Due to Equation (2), yield stress temperature dependence in the monophase area by certain strain rate may be approximated by the exponential function (Figures 1, 2), (9):

$$\sigma_T = \sigma_0^{/} \cdot e^{-b\cdot T} \quad (9)$$

where: $\sigma_0^{/}$ is yield stress under temperature equal 0 K and present strain rate.

The anomaly of the yield stress temperature dependence is case in the temperature range of 500-800 K. There can be seen an athermic area on the diagram of the yield stress temperature dependence or yield stress grows with the temperature. Dynamic strain ageing causes this anomaly. The phase transformation in zirconium alloys occur in the temperature range of 883-1173 K (equilib-

rium conditions) and yield stress temperature dependence becomes non-monotone.

4. Dynamic Strain Ageing

As shown in work [8], yield stress in dynamic strain ageing area can be writing as sum (10):

$$\sigma = \sigma_{adsa} + \sigma_{dsa} \quad (10)$$

where:

σ_{adsa} – yield stress with absence of dynamic strain ageing,

σ_{dsa} –stress caused by dynamic strain ageing.

Let's assume, that (11):

$$\sigma_{dsa} \sim \sigma_{adsa} \quad (11)$$

Then Equation (10) becomes as follows (12):

$$\sigma = \sigma_{adsa} \cdot (1 + F(T, \dot{\varepsilon})) \quad (12)$$

where $F(T, \dot{\varepsilon})$ is some function (13),

$$\sigma_{adsa} = \sigma_0^{/} \cdot \exp(-b \cdot T) \quad (13)$$

where $\sigma_0^{/}$ is yield stress under temperature equal 0 K and present strain rate.

The analysis of existent data given that F-function can be wrote down as follows (14):

$$F(T, \dot{\varepsilon}) = C_{1F} \cdot \exp\left(- \frac{(T - C_{2F} - C_{3F} \cdot \dot{\varepsilon})^2}{C_{4F}} \right) \quad (14)$$

where C_{1F}, C_{2F}, C_{3F}, C_{4F} are constants.

Figure 3 shows the experimental and calculated yield stress data of E110 alloy; F-function temperature dependence is also shown in this figure. The experimental data on the deforming of E635 alloy in dynamic strain ageing temperature area is not enough for defining the F-function.

5. Phase Transformation Influence on Yielding Stress

Figures 4 and 5 show the dependence of the β-phase concentration in E110 and E635 alloys on the temperature.

The phase transformation boundaries shift into the area of higher temperatures with increase of heating rate. The close-packed hexagonal lattice becomes the volume-centered lattice during phase transformation process and this causes changes in mechanical characteristics. Yield stress temperature dependence becomes non-monotone in the area of phase transformation, and so does yielding stress under high plastic strain (Figure 6). Assume that alloy deforming in the two-phase area gives us equal deformations in different phases. Consequently, the yielding stress dependence on the phase concentration can be described by Eq. (15):

$$\sigma(T, \dot{\varepsilon}, \varepsilon) = (1 - \beta(T, \dot{T})) \cdot \sigma_\alpha(T, \dot{\varepsilon}, \varepsilon) + \beta(T, \dot{T}) \cdot \sigma_\beta(T, \dot{\varepsilon}, \varepsilon) \quad (15)$$

where:

$\sigma(T, \dot{\varepsilon}, \varepsilon)$ – yielding stress of two-phase alloy,

$\beta(T, \dot{T})$ – β-phase concentration, which depends on the temperature and heating rate,

$\sigma_\alpha(T, \dot{\varepsilon}, \varepsilon)$ and $\sigma_\beta(T, \dot{\varepsilon}, \varepsilon)$ are α and β – phase yielding stress.

The phase transformation kinetics data are necessary in order to used equation (15).

6. Strain Rate Influence on Yield Stress

The strain rate influence on yield stress can be described by the following Equation (16):

$$\sigma_T = \sigma_0^{//} \cdot \left(\frac{\dot{\varepsilon}}{\dot{\varepsilon}_0} \right)^a \quad (16)$$

where:

$\sigma_0^{//}$ is yield stress by the strain rate – $\dot{\varepsilon}_0$,

$\dot{\varepsilon}_0$ is a certain strain rate, which is a normalization factor.

Usually the normalization factor is equal to least strain rate from the experimental data, in this work it was accepted what

$\dot{\varepsilon}_0 = 1 \cdot 10^{-4}$ c^{-1}.

Figures 7, 8 show the experimental data of strain rate influence on yield stress under different test temperatures, taken under strain rates of $2.5 \cdot 10^{-3}$ c^{-1} and $2 \cdot 10^{-3}$ c^{-1}. The experimental data of yield stress of E635 alloy under temperature higher then 873 K and strain rate equal $2 \cdot 10^{-3}$ c^{-1} is absent.

7. Influence of Deformation Strengthening on Yielding Stress

Due to the Equations (1) and (2) the factor Z_ε is as follows (17):

$$Z_\varepsilon = \frac{\sigma}{\sigma_T} \quad (17)$$

where:

σ – the yielding stress,

σ_T – yield stress.

On other hand, in according to Equation (6),

$Z_\varepsilon = e^{m(1-\eta^\upsilon)}$,

and consequently (18):

$$\frac{\sigma}{\sigma_T} = e^{m(1-\eta^\upsilon)} \quad (19)$$

Figures 9 and 10 show the data of the strengthening of E110 alloy. The data of deforma-

tion strengthening of E635 alloy under high temperatures is not enough for describing the plastic strain of this alloy.

8. Yielding Stress Dependence of E110 Alloy on the Deforming Characteristics

Due to Equations (15), (12) and (1) the alloy yielding stress depends on plastic strain, temperature, heating rate and strain rate as in the following (19):

$$\sigma(T,\dot{\varepsilon},\varepsilon) = (1-\beta(T,\dot{T}))\cdot\sigma_{T\alpha}(T,\dot{\varepsilon})\cdot Z_{\varepsilon\alpha}(T,\dot{\varepsilon},\varepsilon) + \\ + \beta(T,\dot{T})\cdot\sigma_{T\beta}(T,\dot{\varepsilon})\cdot Z_{\varepsilon\beta}(T,\dot{\varepsilon},\varepsilon) \quad (19)$$

where:

$\beta(T,\dot{T})$ is dependence of β-phase concentration on the temperature and the heating rate.

$\sigma_{T\alpha}(T,\dot{\varepsilon})$ and $\sigma_{T\beta}(T,\dot{\varepsilon})$ are yield stresses of α and β-phases, $Z_{\varepsilon\alpha}(T,\dot{\varepsilon},\varepsilon)$ and

$Z_{\varepsilon\beta}(T,\dot{\varepsilon},\varepsilon)$ are deformation strengthening of α and β-phases (20–23):

$$\sigma_{T\alpha}(T,\dot{\varepsilon}) = \sigma_{0\alpha}\cdot\exp(-b_\alpha\cdot T)\cdot\left(\frac{\dot{\varepsilon}}{\dot{\varepsilon}_0}\right)^{C_{1a\alpha}+C_{2a\alpha}\cdot T}\cdot \\ \cdot\left(1+C_{1F}\cdot\exp\left(-\frac{(T-C_{2F}-C_{3F}\cdot\dot{\varepsilon})^2}{C_{4F}}\right)\right) \quad (20)$$

$$\sigma_{T\beta}(T,\dot{\varepsilon}) = \sigma_{0\beta}\cdot\exp(-b_\beta\cdot T)\cdot\left(\frac{\dot{\varepsilon}}{\dot{\varepsilon}_0}\right)^{C_{1a\beta}+C_{2a\beta}\cdot T} \quad (21)$$

$$Z_{\varepsilon\alpha}(T,\dot{\varepsilon},\varepsilon) = \exp\left(\begin{array}{l}(C_{1m\alpha}+C_{2m\alpha}\cdot T)\cdot\left(1+C_{3m\alpha}\cdot\lg\left(\frac{\dot{\varepsilon}}{\dot{\varepsilon}_0}\right)\right)\cdot \\ \cdot\left(1-(1+\varepsilon)^{C_{1v\alpha}\cdot\left(\frac{\dot{\varepsilon}}{\dot{\varepsilon}_0}\right)^{C_{2v\alpha}}}\right)\end{array}\right) \quad (22)$$

$$Z_{\varepsilon\beta}(T,\dot{\varepsilon},\varepsilon) = \exp\left(\begin{array}{l}(C_{1m\beta}+C_{2m\beta}\cdot T)\cdot(1+C_{3m\beta}\cdot\lg(\frac{\dot{\varepsilon}}{\dot{\varepsilon}_0})) \\ \cdot\left(1-(1+\varepsilon)^{C_{1v\beta}\cdot\left(\frac{\dot{\varepsilon}}{\dot{\varepsilon}_0}\right)^{C_{2v\beta}}}\right)\end{array}\right) \quad (23)$$

The coefficients for the equations (20)–(23) for E110 alloy were defined using available experimental data. As there is not enough data concerning the influence imposed by the heating rate on the phase concentration of E110 alloy, one can only make calculations for low heating rates, using data on the phase concentration of this alloy in equilibrium conditions. Figures 11 and 12 show the calculation results and the experimental yield stress of E110 alloy under the strain rate $2\cdot10^{-3}$ c^{-1}, $2\cdot10^{-3}$ c^{-1}. Figure 13 shows the calculation results and experimental deformation strengthening of E110 alloy under the strain rate $2\cdot10^{-3}$ c^{-1} and the temperature 1073 K. The calculated curves are in good agreement with the experimental data.

Coefficients $\sigma_{0\alpha}$ and $\sigma_{0\beta}$ in Equations (20) and (21) depend on manufacturing technology, metal impurity concentration etc. In each case they are calculated using the formulas (24,25):

$$\sigma_{0\alpha} = \sigma_{T\alpha}(T_\alpha,\dot{\varepsilon})\cdot\exp(b_\alpha\cdot T_\alpha)\cdot\left(\frac{\dot{\varepsilon}}{\dot{\varepsilon}_0}\right)^{-(C_{1a\alpha}+C_{2a\alpha}\cdot T_\alpha)}\cdot \\ \cdot\left(1+C_{1F}\cdot\exp\left(-\frac{(T_\alpha-C_{2F}-C_{3F}\cdot\dot{\varepsilon})^2}{C_{4F}}\right)\right)^{-1} \quad (24)$$

$$\sigma_{0\beta} = \sigma_{T\beta}(T_\beta,\dot{\varepsilon})\cdot\exp(b_\beta\cdot T_\beta)\cdot\left(\frac{\dot{\varepsilon}}{\dot{\varepsilon}_0}\right)^{-(C_{1a\beta}+C_{2a\beta}\cdot T_\beta)} \quad (25)$$

where:

$\sigma_{T\alpha}(T_\alpha,\dot{\varepsilon})$ is a certain yield stress in the α – phase area under the test temperature T_α and the strain rate $\dot{\varepsilon}$;

$\sigma_{T\beta}(T_\beta,\dot{\varepsilon})$ is a certain yield stress in the β – phase area under the test temperature T_β and the strain rate $\dot{\varepsilon}$.

The calculations of the yield stress and the ultimate stress for the four types of circumferential specimens of E110 alloy were carried out. Specimens were made of different types of cladding (Table 1). The calculation results are shown in the Figures 14-17. The calculation results are in good agreement with the experimental data.

9. Conclusions

1. The method for the description of the plastic deformation process in zirconium alloys under designed accident conditions were proposed.
2. On the basis of the experiments made and the existent experimental data the dependence of yielding stress on plastic strain, strain rate, temperature and heating rate for E110 alloy was determined.
3. In future the following research work shall be made:

- Research of dynamic strain ageing in E635 al-

loy under different strain rates.
- Research of strain rate Influence on plastic strain in E635 alloy under test temperature higher than 873 K.
- Research of deformation strengthening of E635 alloy under high temperatures.
- Research of heating rate Influence n phase transformation in E110 and E635 alloys.

References

[1] Yu. Bibilashvily, N. Sokolov, A. Salatov, L. Andreyeva-Andrievskaya, O. Nechaeva, F. Vlasov. RAPTA-5 Code: Modelling of Behaviour of Fuel Elements of VVER Type in Design Accidents. Verification Calculations. Proceedings of IAEA Technical Committee on Behaviour of LWR Core Materials under Accident Conditions, held in Dimitrovgrad, Russia, 9–13 October 1995. IAEA-TECDOC-921, Vienna, 139–152, 1996.

[2] М. Зайков. Режимы деформации и усилия при горячей прокатке. Свердловск: Металлургиздат, 1960.

[3] Л. Лошманов, П. Федотов, Ю. Бибилашвили, О. Нечаева, А. Салатов. Механические свойства сплава Э-635 при динамическом деформировании. Научная сессия МИФИ-2001. Сборник научных трудов. В 14 томах. Т.8: Молекулярная физика. Нетрадиционная энергетика. Ядерная энергетика. М.: МИФИ, 2001,176 с.

[4] Л. Лошманов, П. Федотов, А. Гончаров, О. Нечаева, А. Салатов. Экспериментально-расчетное моделирование поведения оболочек твэлов реакторов типа ВВЭР в условиях быстроизменяющегося температурно-силового нагружения, характерного для первой стадии МПА. Научная сессия МИФИ-2002. Сборник научных трудов. В 14 томах. Т.8: Нетрадиционная энергетика. Ядерная энергетика. М.: МИФИ. 196, 2002

[5] А. Гончаров, О. Нечаева, А. Салатов, П. Федотов. Экспериментально-расчетное моделирование поведения оболочек твэлов реакторов типа ВВЭР в условиях быстро изменяющегося температурно-силового нагружения. Вторая Российская конференция Обеспечение безопасности АЭС с ВВЭР. Сборник трудов. Том 4. Подольск. 2001 г.

[6] Л. Артюхина, В. Зарубин, В. Конопленко, Л. Любимова, Е. Пирогов, Ю. Бибилашвили, И. Головнин, В. Новиков Исследование механических свойств циркониевых сплавов при высоких температурах. В сб. Физика и механика деформации и разрушения. Вып. 9. Прочность материалов и конструкций атомной техники. М.: Энергоиздат, 1981.

[7] В. Панкратов, В. Конопленко, П. Прасолов. Исследование механических свойств и пластической анизотропии сплавов Н-1 и Н-2,5 в диапазоне температур 293-1300 К. В сборнике научных трудов МИФИ: Пластичность, прочность и сопротивление разрушению материалов и элементов ядерных энергетических установок. М. Энергоатомиздат. 1988.

[8] S. Hong, W. Ryu, C. Rim. Elongation Minimum and Strain Rate Sensitivity Minimum of Zircaloy-4. Journal of Nuclear Materials 116. 1983.

[9] А. Займовский, А. Никулина, Н. Решетников. Циркониевые сплавы в ядерной энергетике. 2-е изд., перераб. и доп. М.: Энергоатомиздат. 256, 1994.

[10] T. Forgeron et al. Experiment and Modeling of Advanced Fuel Rod Cladding Behavior Under LOCA Conditions: Alpha-Beta Phase Transformation Kinetics and EDGAR Methodology. Authorized reprint from standard technical publication1354 @ Copyright 2000, Zirconium in the nuclear industry: Twelfth Symposium, American Sosiety for Testing and Materials, 100 Barr Harbor Drive, West Conshohocken, PA 19428–2959.

[11] Е. Пирогов, А. Анкудинов, О. Комаров и др. Исследование и прогнозирование деформационного повеления оболочечных материалов при быстром нагреве. – Радиационное материаловедение. Харьков. 1991. т.8.

[12] Г. Кобылянский, А. Новоселов. Радиационная стойкость циркония и сплавов на его основе. Справочные материалы по реакторному материаловедению. Димитровград 1996.

Table 1. E110 alloy specimens for comparatives calculations [12]

Type	Description		$\dot{\varepsilon}$, c^{-1}	$\sigma_{0\alpha}/\sigma_{0\beta}$, [MPa]	ε_p^{**}
1	Article Thermal treatment Size of specimen, [mm] Hydrogen concentration, [%]	Fuel road cladding (WWER) Annealing during 3 hour under 853 K 9.15×0.7×2.8* 0.01-0.03	$2 \cdot 10^{-3}$	844/20.1	0.088-0.174
2	Article Thermal treatment Size of specimen, [mm] Hydrogen concentration, [%]	Fuel road cladding (RBMK) Annealing during 3 hour under 853 K 13.6×0.9×3.0 -	$2 \cdot 10^{-3}$	785/-	0.087-0.32
3	Article Thermal treatment Size of specimen, [mm] Hydrogen concentration, [%]	Tube Annealing during 2 hour under 853 K 5.8×0.5×2.5 0.002-0.010	$7 \cdot 10^{-3}$	655/-	0.07-0.131
4	Article Thermal treatment Size of specimen, [mm] Hydrogen concentration, [%]	Tube Annealing during 2 hour under 853 K 8.0×0.5×2.8 0.006	$2.6 \cdot 10^{-3}$	684/-	0.055-0.131

* External diameter × wall thickness × ring height

** $\varepsilon_P = \ln(1+\delta_P)$, where δ_P – uniform elongation

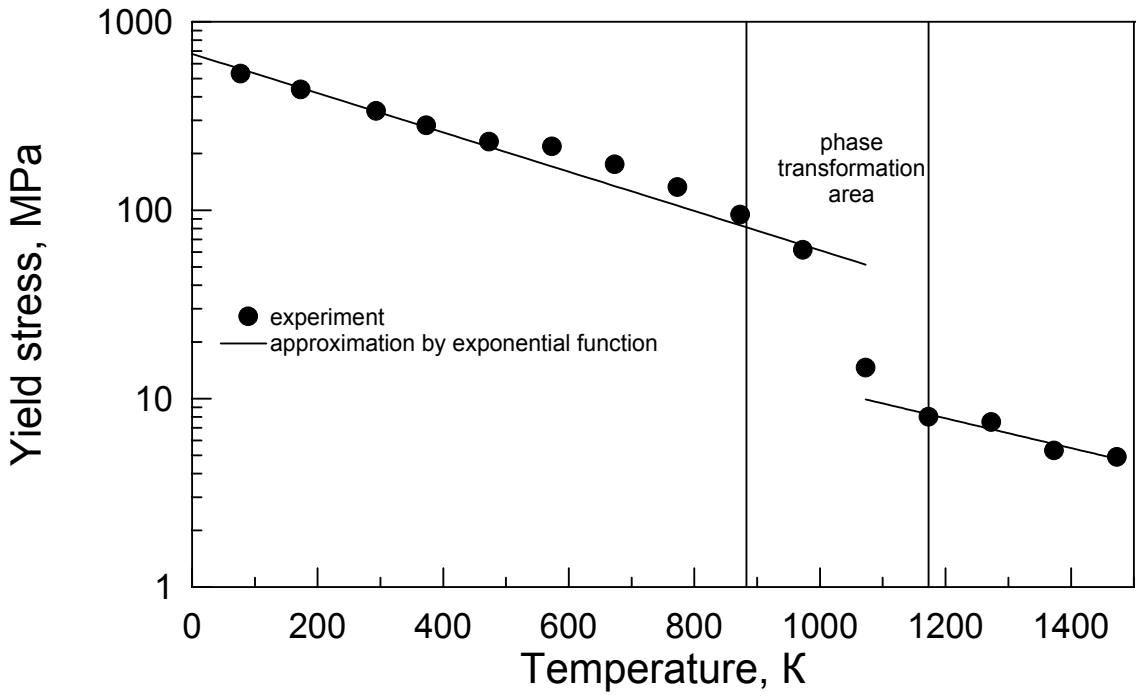

Figure 1. Yield stress of E110 alloy

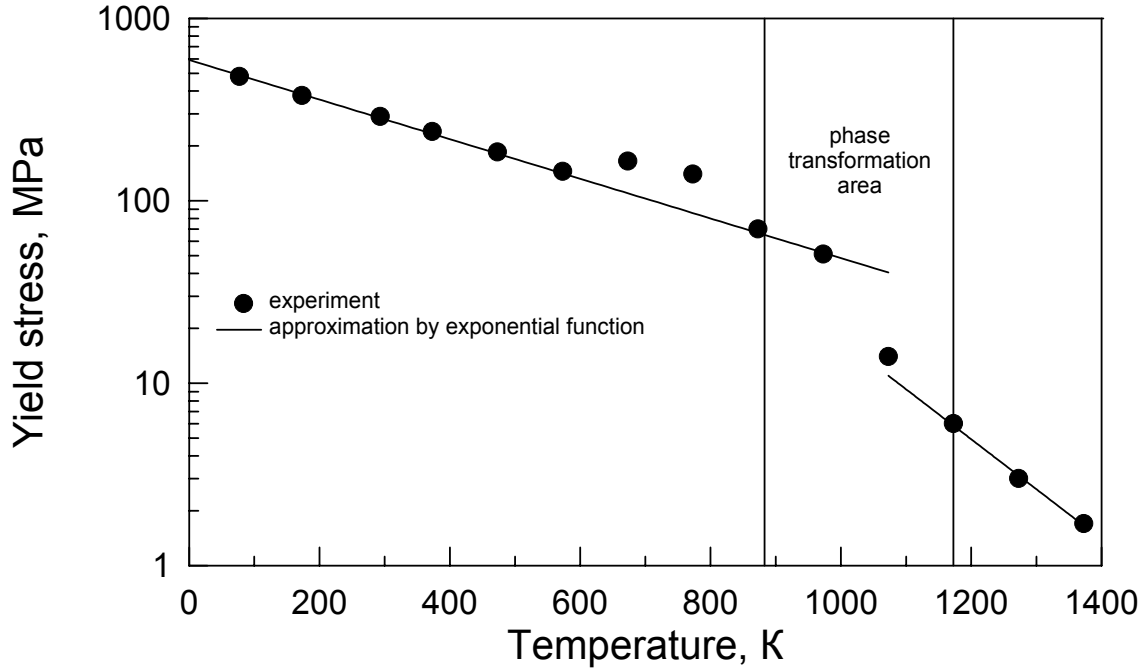

Figure 2. Yield stress of E635 alloy

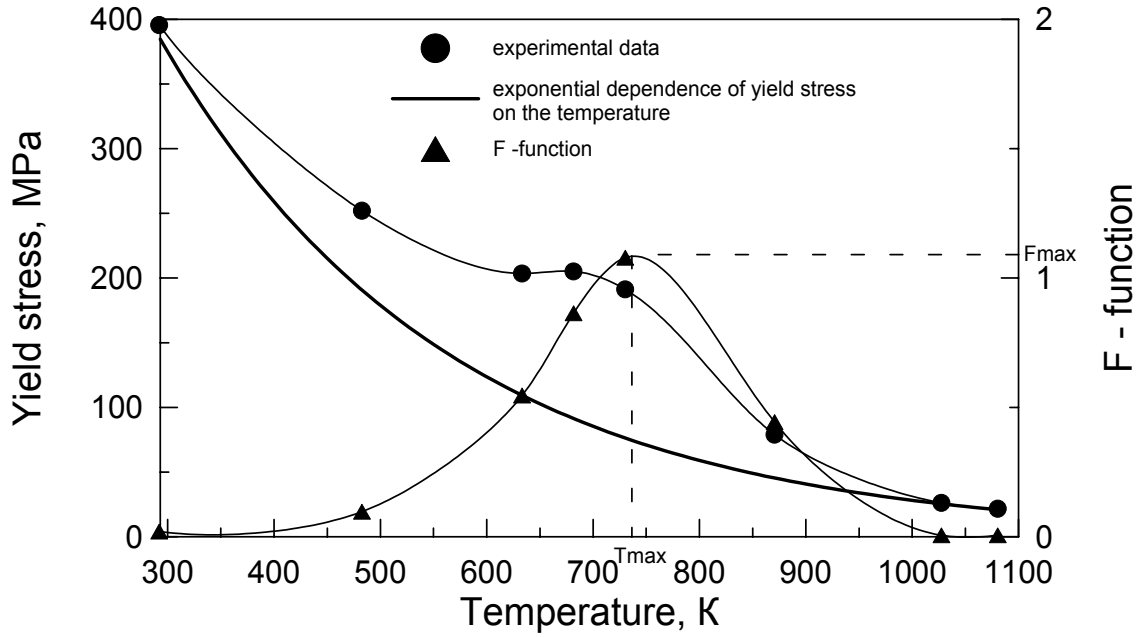

Figure 3. Dynamic strain ageing effect in E110 alloy

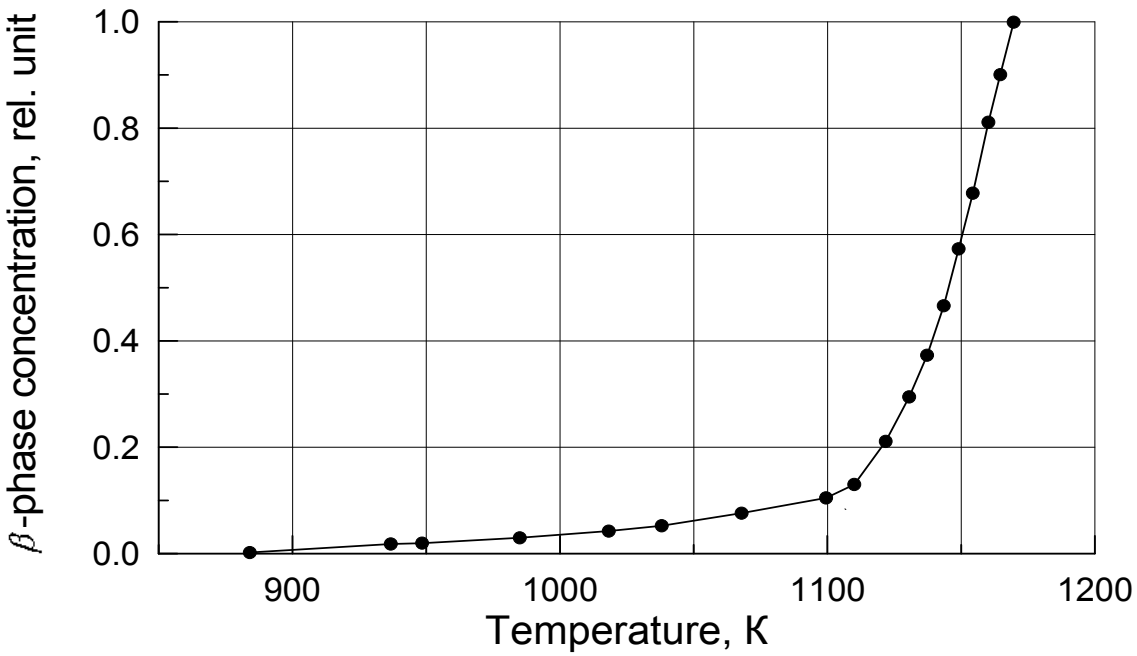

Figure 4. β-phase concentration in E110 alloy

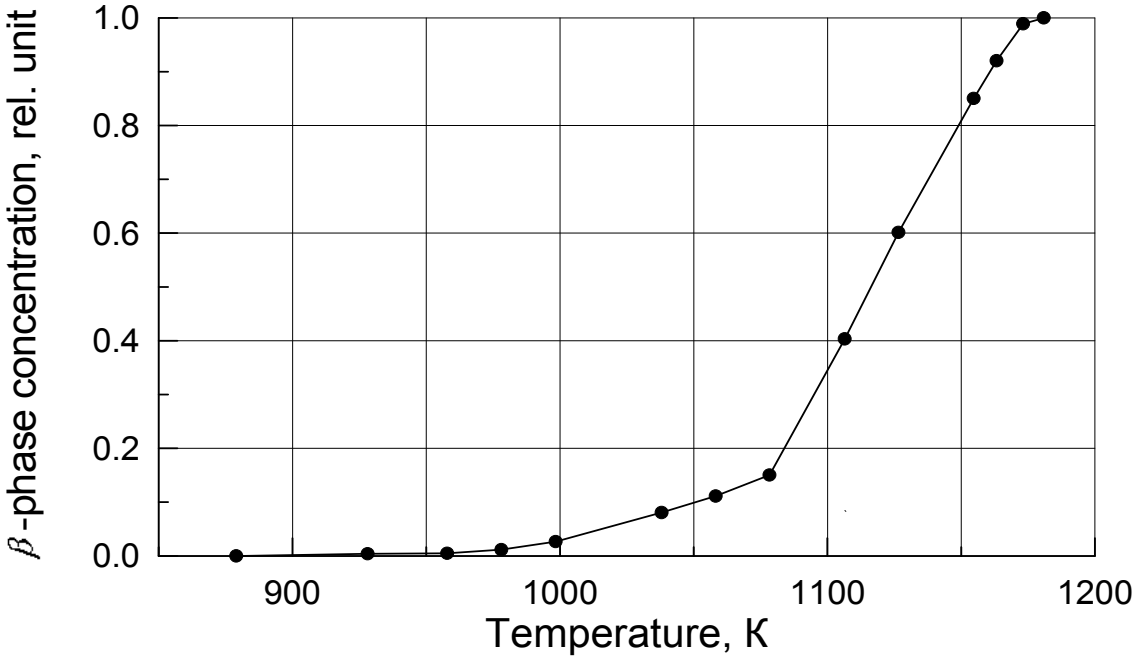

Figure 5. β-phase concentration in E635 alloy

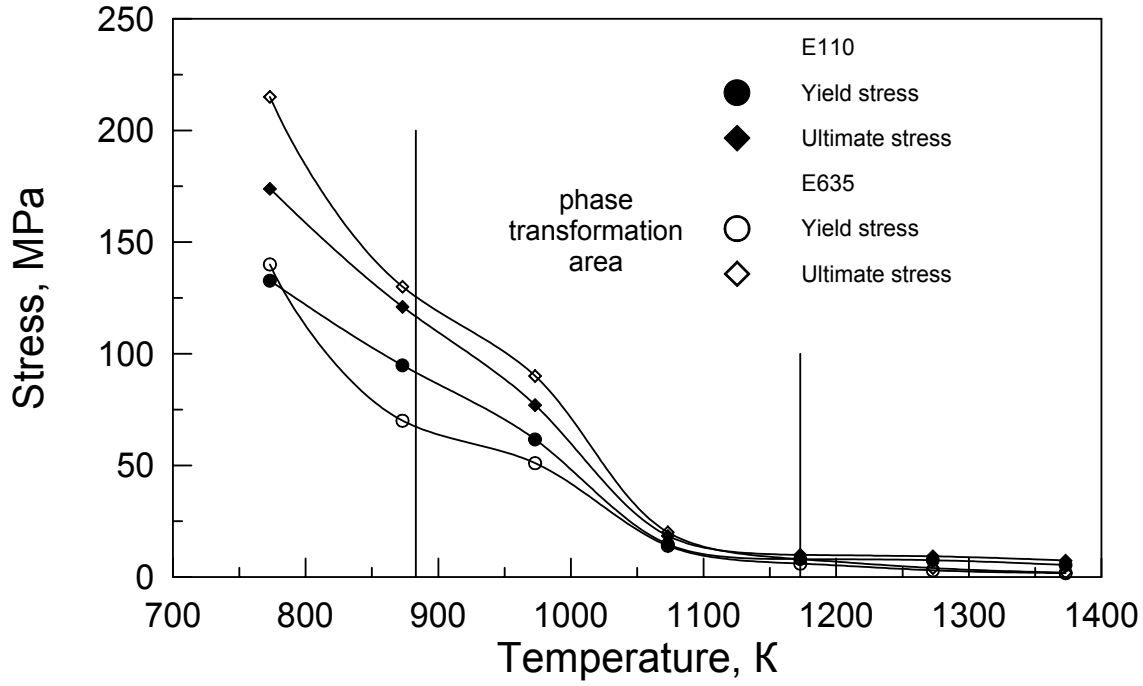

Figure 6. Strength properties of E110 and E635 alloys

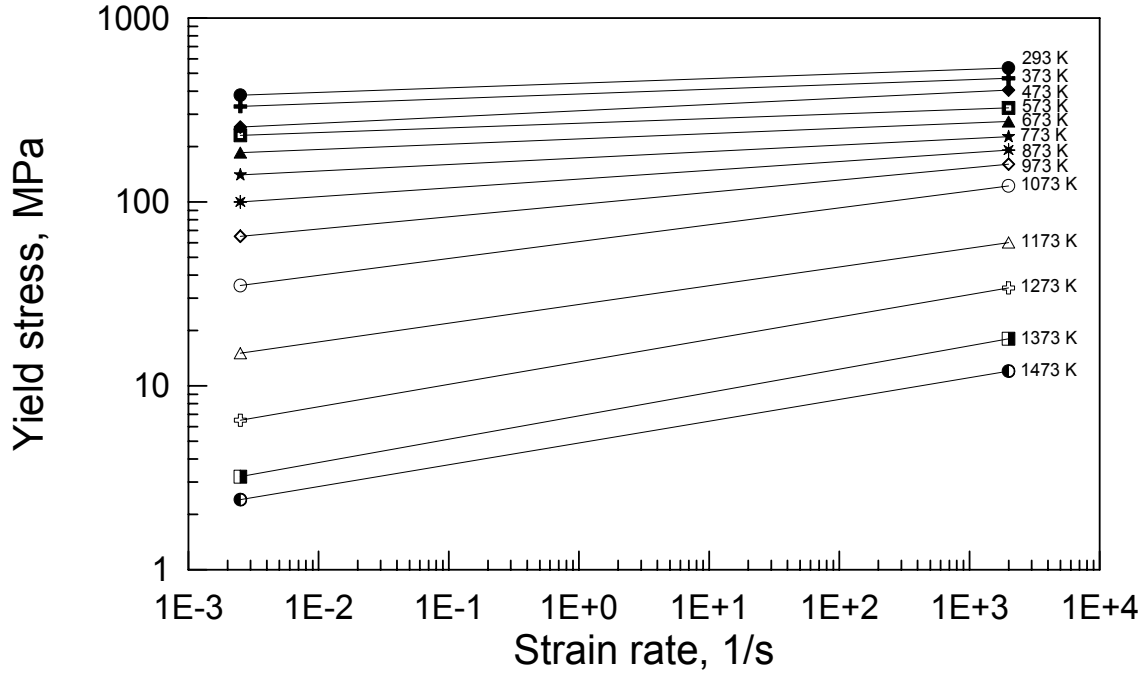

Figure 7. Strain rate influence on yield stress of E110 alloy

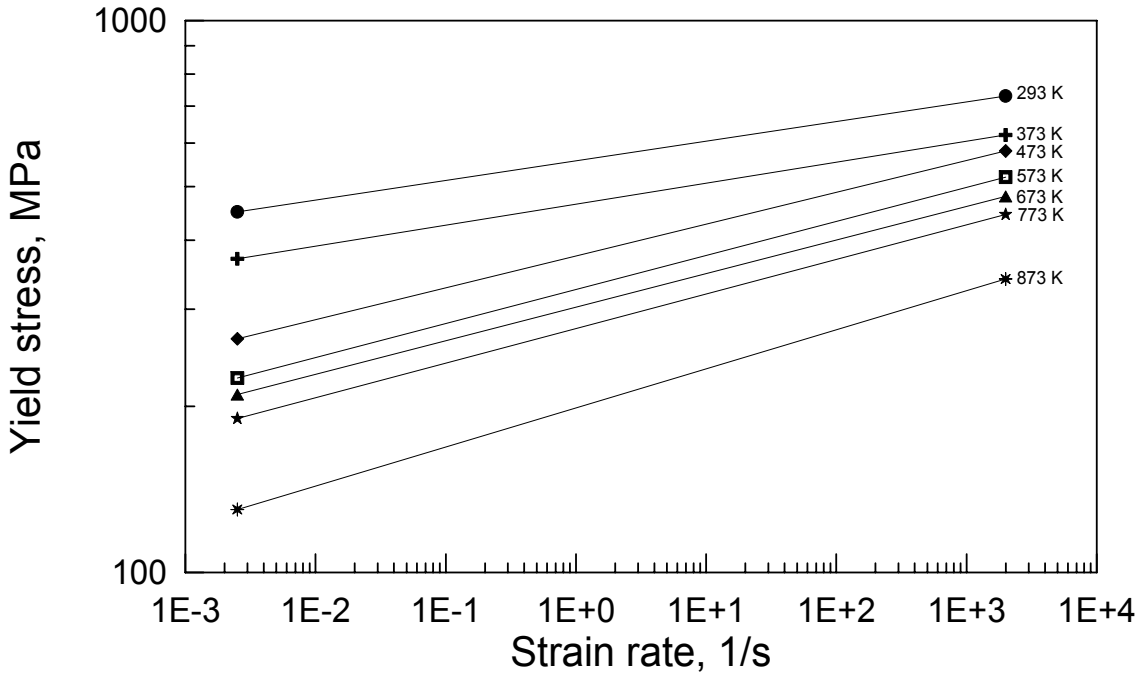

Figure 8. Strain rate influence on yield stress of E635 alloy

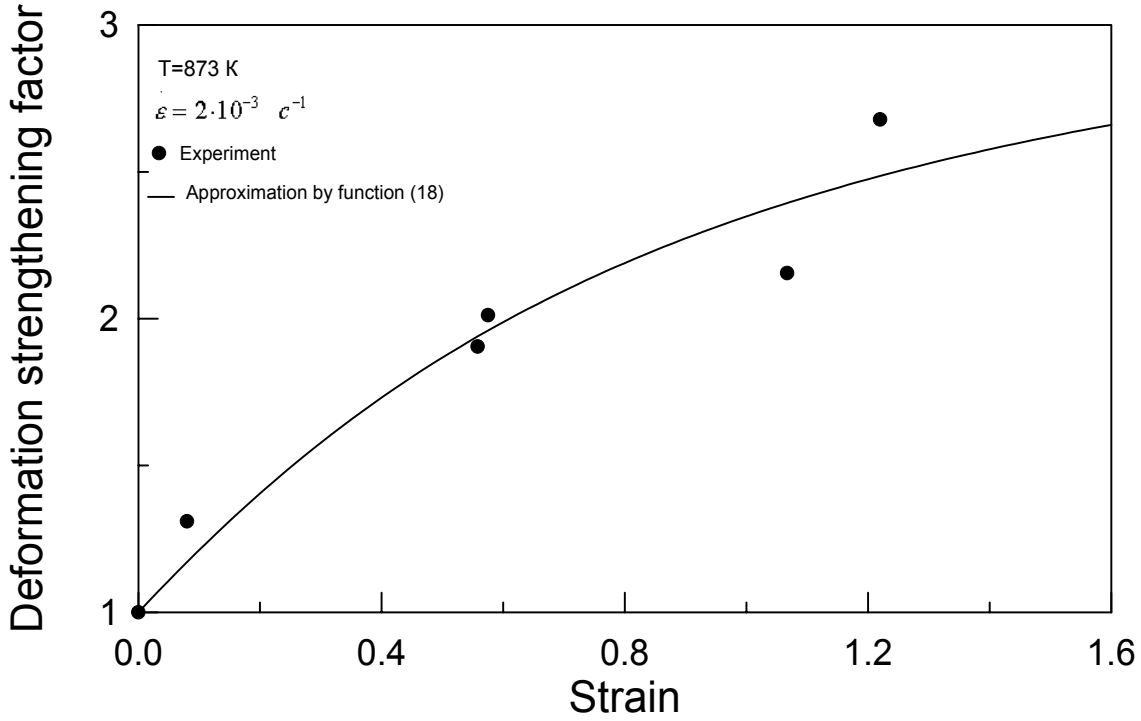

Figure 9. Strengthening of E110 alloy under temperature of 873 K

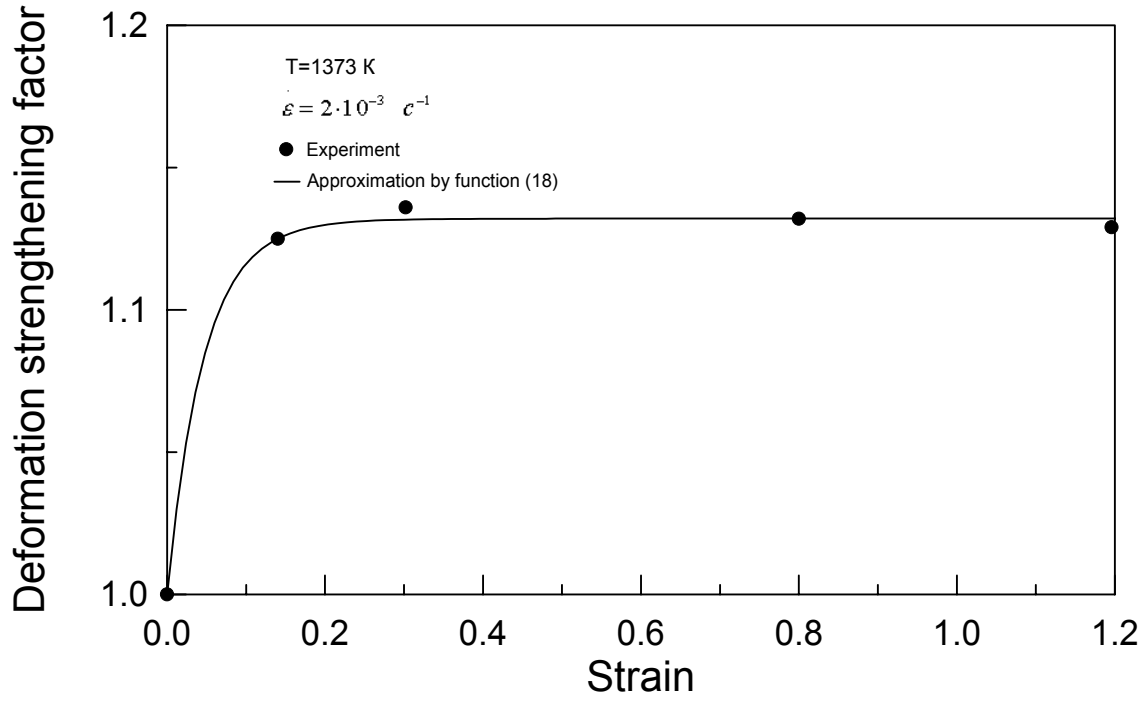

Figure 10. Strengthening of E110 alloy under temperature of 1373 K

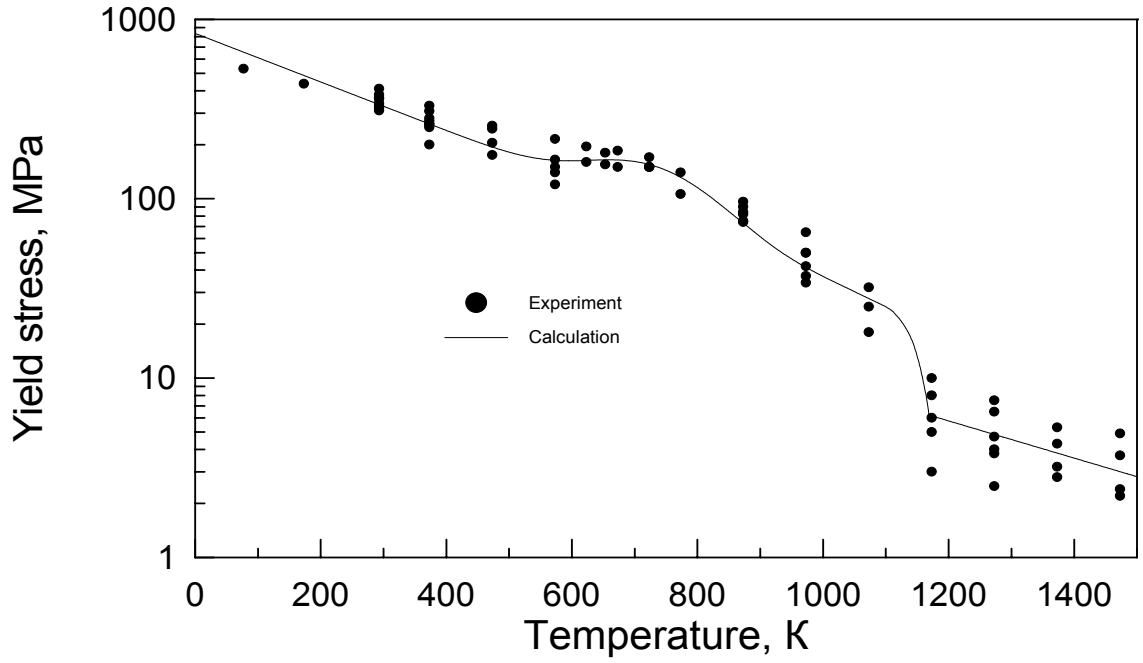

Figure 11. Yield stress of E110 alloy versus temperature under strain rate $2 \cdot 10^{-3}$ c^{-1}

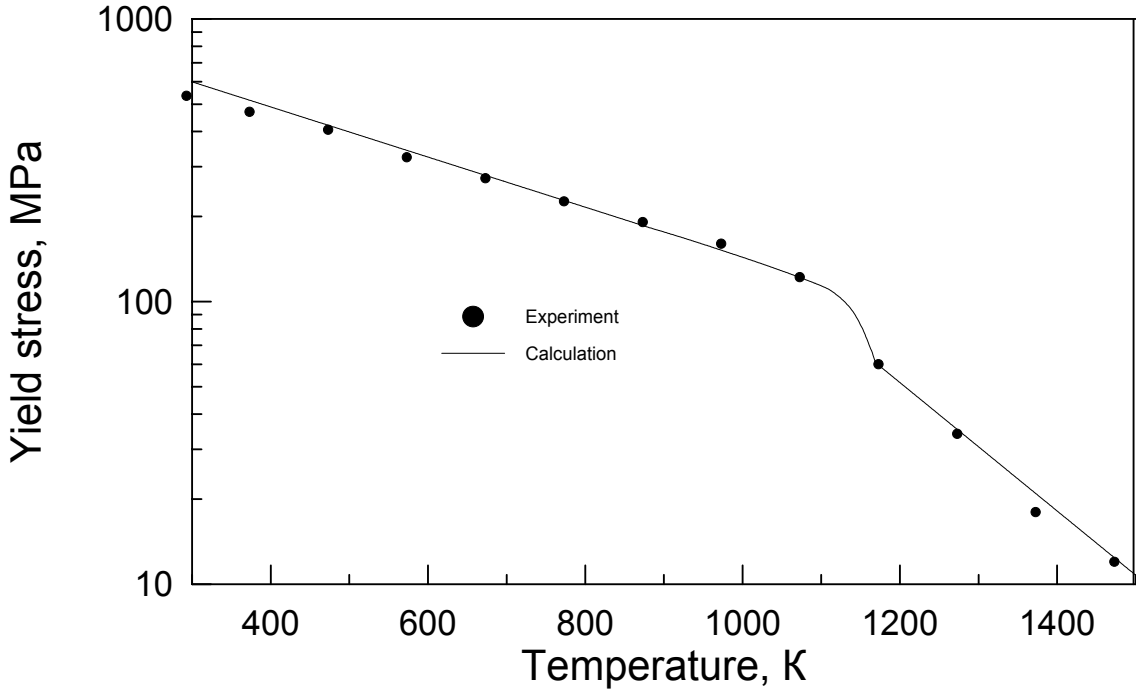

Figure 12. Yield stress of E110 alloy versus temperature under strain rate $2 \cdot 10^{-3}$ c^{-1}

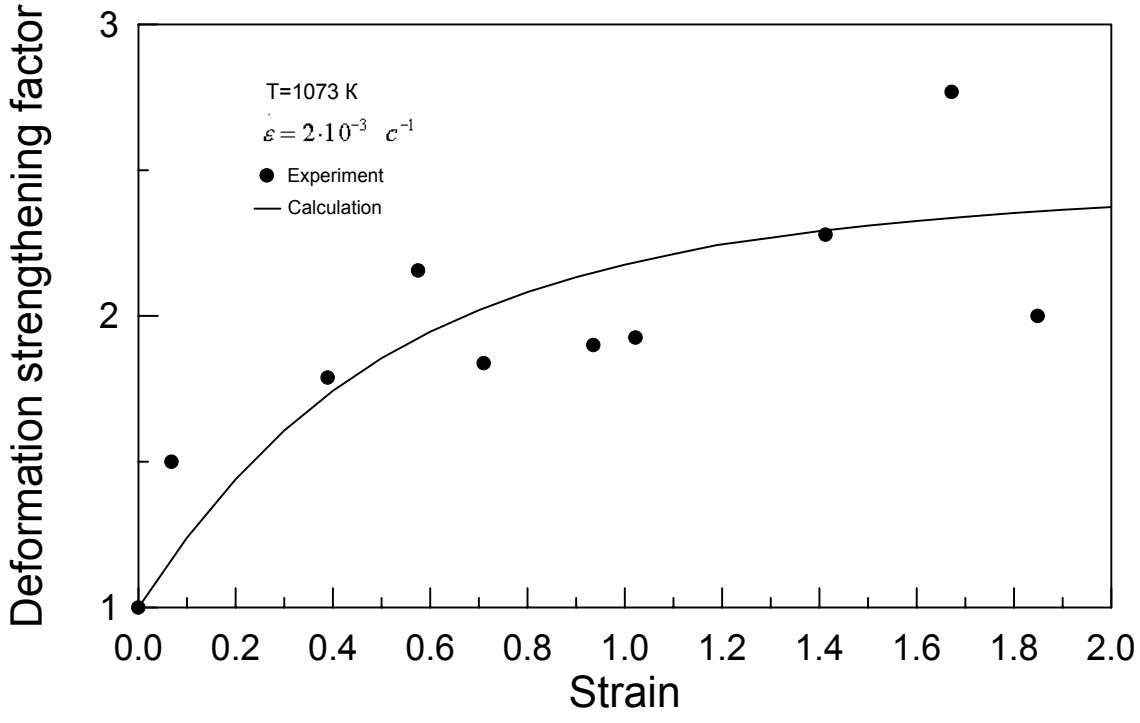

Figure 13. Strengthening of E110 alloy under temperature of 1073 K

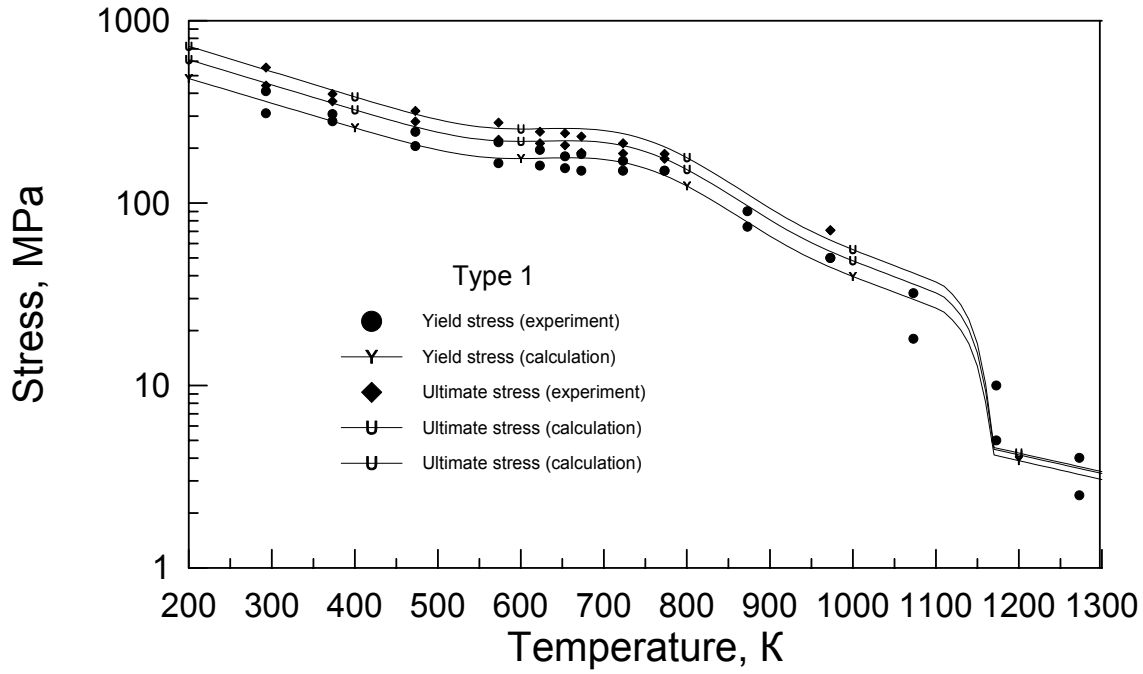

Figure 14. Yielding stress of circumferential specimens of E110 alloy versus temperature (type 1)

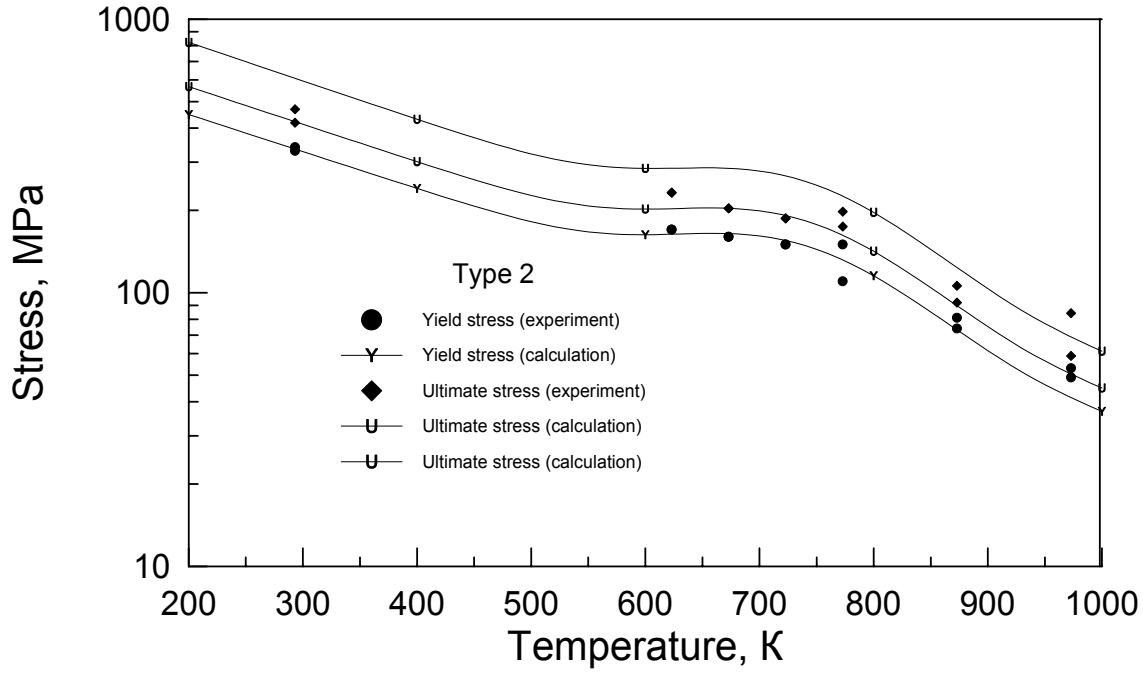

Figure 15. Yielding stress of circumferential specimens of E110 alloy versus temperature (type 2)

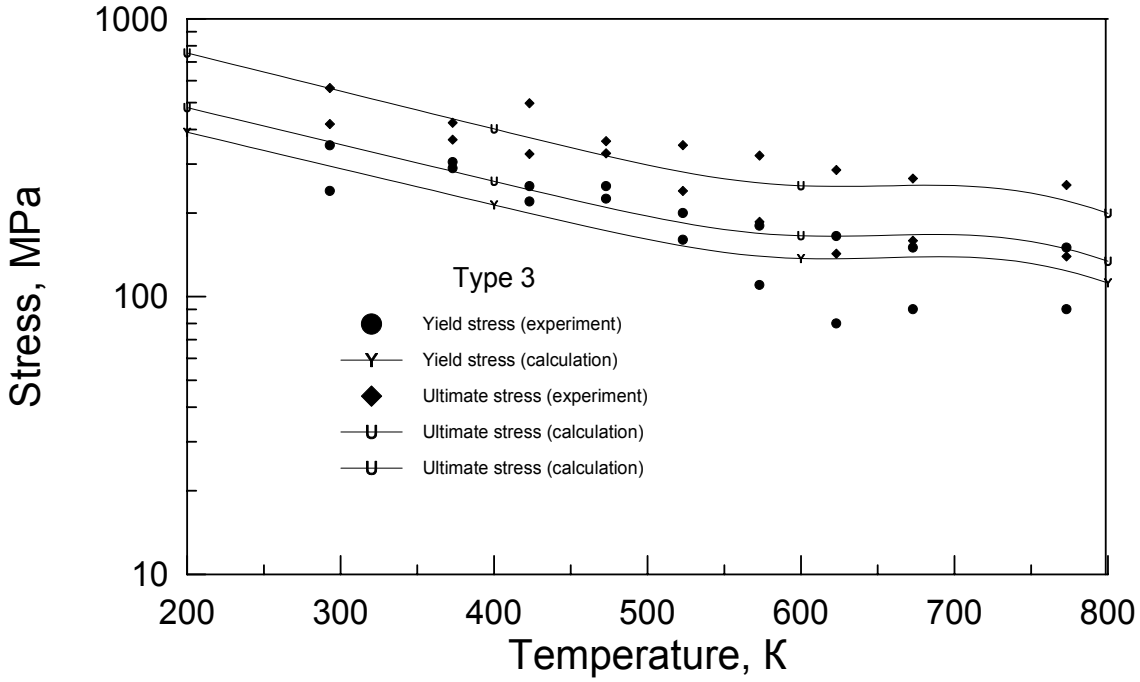

Figure 16. Yielding stress of circumferential specimens of E110 alloy versus temperature (type 3)

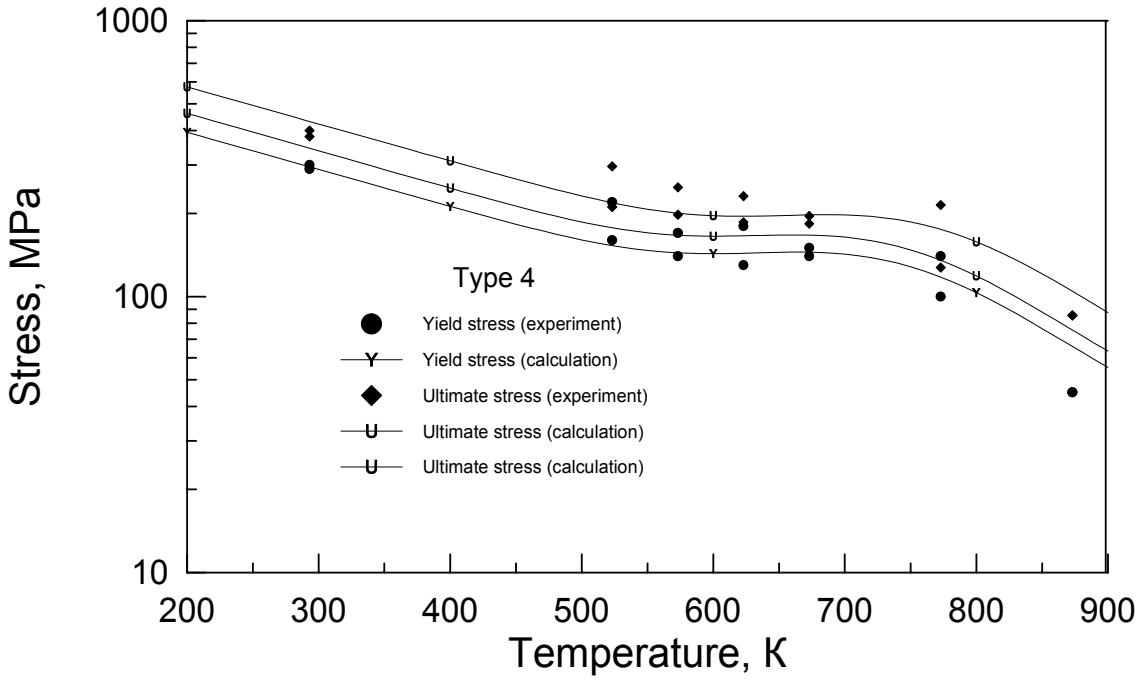

Figure 17. Yielding stress of circumferential specimens of E110 alloy versus temperature (type 4)